GEOPHYSICS, VOL. 38, NO. 2 (APRIL 1973), P. 339–348, 11 FIGS.

EQUIVALENT SOURCES USED AS AN ANALYTIC BASE FOR PROCESSING TOTAL MAGNETIC FIELD PROFILES†

DAVID A. EMILIA*

Equivalent sources are useful in processing total magnetic field profiles. A lines-of-dipoles distribution, obtained by solving the linear inverse problem, provides an analytic base for computing the following quantities from an observed field: first and second vertical derivative fields, upward- and downward-continued fields, field reduced to the pole, amplitude spectrum of the field, and band-passed field. A theoretical example demonstrates the validity of the approach, and a field example shows that reasonable results are readily obtained.

INTRODUCTION

Solutions to the inverse problem of potential theory have been presented and extensively discussed by many authors (e.g., Hall, 1958; Corbato, 1965; Hahn, 1965; Zidarov, 1965; Bott, 1967; Johnson, 1969; Emilia and Bodvarsson, 1969; Bodvarsson, 1971). The object of these papers is to provide geologically and geophysically feasible interpretations of observed potential field anomalies. Recently Dampney (1969) and Needham (1970) have shown that equivalent sources, obtained as solutions to the inverse gravity problem, can be used to further process the observed gravity field. In both papers the theoretical field of a distribution of point masses, computed on the basis of the original field observations, is used to analytically determine those observations on a different surface.

Potential fields can be extensively processed using equivalent source solutions of the inverse problem. In particular, the pertinent analytic equation as obtained from a final equivalent source distribution is used to calculate each of the following quantities directly from the observed total magnetic field: first and second vertical derivative fields, upward- and downward-continued fields, field reduced to the pole, amplitude spectrum of the field, and band-passed field. Other quantities such as horizontal and vertical field components, higher-order vertical derivatives, horizontal derivatives, and power and phase spectra may be calculated using the equivalent-source technique, but they are not considered further.

THE METHOD

The inverse problem of potential theory, in its general form, involves direct use of field observations to estimate parameters that describe an acceptable source configuration; the theoretical field of a model source configuration is a linear function of the magnitude parameter (e.g., mass or magnetization amplitude) and a nonlinear function of the source location and geometry. One of many algorithms available is used to iteratively adjust an initially assumed set of source-body parameters, and formal acceptance of a set of parameters depends on whether it gives the particular "fit" required between the theoretical and observed fields.

The ambiguity in modeling potential fields is quite evident when solving the inverse problem. The final set of parameters describing a source configuration depends on the initially assumed set of variable parameters. In turn, the initial model depends on the purpose of the individual study and whether known geological and geophysical data are used as constraints. We are not concerned with physical ambiguity, that is, the physi-

† Manuscript received by the Editor March 31, 1972; revised manuscript received August 26, 1972.

* Marathon Oil Company, Littleton, Colorado; now with Pacific Oceanographic Laboratory, NOAA, Seattle, Washington 98195.

cal correctness of the final source distribution, but with the stability of that source distribution and the reliability of the agreement between the theoretical field and the observed field. The concepts of reliability and stability are discussed extensively in the above references and by other authors (Bullard and Cooper, 1948; Strakhov, 1969; Bott and Hutton, 1970a, b; Emilia and Bodvarsson, 1970). It suffices to say here that the source distribution shows instabilities if it is too far below the level of observation, and interpolated amplitudes of the theoretical field become quite unrealistic if the source distribution is too shallow with respect to the sampling interval of the observed field.

For the theoretical example used in this paper, a total magnetic field profile observed on a plane is approximated by the total magnetic field of a distribution of infinite lines of magnetic dipoles perpendicular to the profile and located on a plane parallel to the plane of observations. Line-of-dipole equations for the quantities mentioned in the Introduction are presented in the Appendix. All physical sources are assumed to be two-dimensional and perpendicular to the observed profile. Total-field anomalies may be processed using equivalent sources if they are assumed to be much less than the regional geomagnetic field, thus allowing that observed quantity to take on the analytic properties of a potential field (Henderson, 1970).

It is not necessary to solve a general nonlinear inverse problem to obtain a suitable system of lines of dipoles. We therefore formulate the linear problem by fixing the location of each of the lines of dipoles and varying just the individual dipole moments per unit length; this is equivalent to the procedure of Dampney (1969) where the mass of each individual point mass is varied. The Marquardt algorithm for iterative estimation of source parameters (see Johnson, 1969) is used, and the digitized field of our final distribution of lines of dipoles agrees with the digitized observed field in a least-squares sense. Upon obtaining such a fit we can, as discussed above, analytically process the observed field.

THEORETICAL EXAMPLE

The object of this section is to show how the quantities obtained from a theoretical field using the equivalent source technique agree with the known analytical quantities. The basic theoretical model used here is a two-dimensional, uniformly magnetized (1 ampere/meter MKSA or 0.001 emu/cm^3) rectangular prism centered at the origin and striking 40 degrees with respect to geographic north; it is 7-km thick and 12-km wide with its top at a depth of 3 km (Figure 1). Induced magnetization with inclination 68°N and declination 8°W is assumed. The theoretical input field is digitized every 2 km from -50 to 50 km, and a line of dipoles with the same induced magnetic properties as the prism is located 4 km under each "point of observation." This latter fact allows excellent agreement between the lines-of-dipoles field and the "observed" field at each point of observation.

In Figure 1 the theoretical field and the field due to the final distribution of lines of dipoles are shown to overlie one another. Both fields are calculated every 1 km to show the quality of the interpolation points and to confirm that the lines of dipoles are not too shallow. Note that the lines-of-dipoles field is also calculated beyond ± 50 km to show that no spurious oscillations occur there; the final dipole moments per unit length (not shown) showed no significant instabilities. The first vertical derivative calculations are also compared in Figure 1, and they agree quite well. We therefore expect similar agreement when the second vertical derivative fields, the upward-continued (5 km) fields, and the downward-continued (1 km) fields are compared. This is indeed the case, as shown in Figures 2 and 3. In this test case, agreement between downward-continued fields starts to deteriorate at a downward-continuation depth of about 2 km. Again, all fields have been calculated at 1-km intervals to demonstrate interpolation reliability.

The total magnetic field reduced to the pole is by definition the field that would be observed if all the source bodies were located at the geomagnetic pole and had vertical magnetization (Baranov, 1957; Bhattacharyya, 1965). To obtain such a reduction using the analytic equation for the field of the final equivalent source distribution, we merely change the inclinations of the dipole moment per unit length and the geomagnetic field to 90 degrees and recalculate the total field. The result obtained from a distribution of lines of dipoles with correctly assumed magnetic inclination (induced) is shown in Figure 2; it is identical to the theoretical field at the pole. However, if the magnetization direction of the model

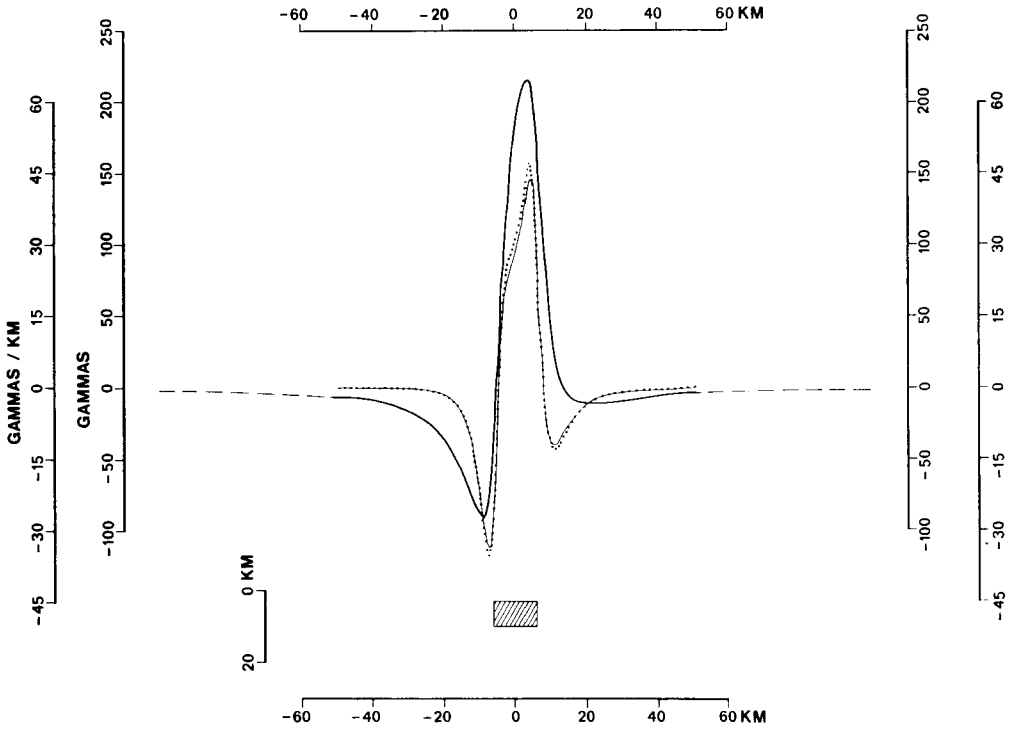

FIG. 1. Hachured block represents the two-dimensional rectangular prism used in theoretical example. Thick solid line is total magnetic field due to prism; dashed line (mostly obscured by prism field) is total magnetic field due to final lines-of-dipoles distribution as obtained by solution of the inverse magnetic problem. Thin solid line is first vertical derivative field due to prism; dotted line is first vertical derivative field due to final lines-of-dipoles distribution.

prism is not the same as that of our equivalent source distribution, then the calculated field at the pole is incorrect. This is shown in Figure 2 by the dashed profile; it was obtained by an equivalent-source distribution with induced inclination and declination of 68°N, 8°W from the field of a model prism with regional field inclination and declination of 68°N, 8°W and remanent-magnetization inclination and declination of 60°N, 25°W. Bhattacharyya (1965) gives a very good discussion of the problems involved in assuming correct magnetic direction for reduction-to-the-pole calculations. Note that the derivative fields and the continued fields obtained in this latter case are correct because the potential field behavior does not depend on the directional properties of the equivalent magnetic sources involved.

The analytic equation (A4) for the amplitude spectrum of the field due to a distribution of lines of dipoles is obtained quite easily from the analytic equation for the Fourier transform of that field. In Figure 4 the amplitude spectrum of the test field as obtained from a standard fast Fourier transform technique is compared to that obtained from our final lines-of-dipoles distribution; both spectra are normalized to unity and essentially overlie one another. Also shown in Figure 4 is the amplitude spectrum of the downward-continued field (Figure 3) as obtained from the final lines-of-dipoles distribution; note the expected increase in the higher frequency content of that downward-continued field.

The analytic equation for a band-passed, lines-of-dipoles field is obtained by analytically calculating its inverse Fourier transform between the band-pass frequency limits, instead of between minus and plus infinity [see equation (A5)]. For the theoretical example under consideration, those frequencies corresponding to the smaller lobe in Figure 4 can be eliminated by using low-pass limits of 0 and 0.08 cycles/km. The result is shown in Figure 5 along with the difference be-

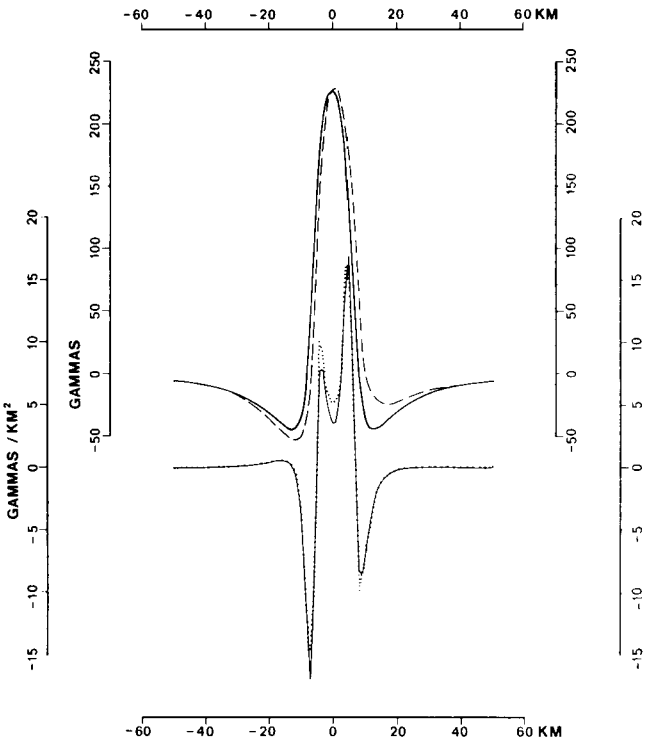

FIG. 2. Thick (uppermost) solid line represents three fields: the field at the pole of the prism with either induced or remanent magnetization and the field at the pole of the final lines-of-dipoles distribution with correctly assumed (induced) magnetization properties. The dashed line is the field at the pole of the final lines-of-dipoles distribution with induced magnetic properties, as obtained from the field of a prism with dominant remanent magnetization (see text).

Thin solid line is second vertical derivative field due to prism. Dotted line is second vertical derivative field due to final lines-of-dipoles distribution.

tween it and the original field; standard fast Fourier transform filtering yields the same low-pass field. The amplitude spectrum (obtained by a standard fast Fourier transform technique) of the final low-pass field is shown by the dotted line in Figure 4.

FIELD EXAMPLE

A total-field anomaly profile from the continental rise region off Cape Hatteras has been subjected to some of the operations described above to provide an example of the type of results obtained from field data; no "best" geologic geophysical interpretation is attempted. The profile, which appears in Brakl et al (1968) and more recently in Emilia et al (1972) has been digitized every 5.35 km. Induced magnetic properties are assumed, and the inclination, declination, and strike are identical to those used in the above theoretical example. A line of dipoles was placed under each digitized field value at a depth of 12 km.

In Figure 6 the field profile is overlain by the lines-of-dipoles field (calculated every 2.675 km). Interpolation is generally good when compared to the linearly interpolated values; however, the larger discrepancies around the 280-km point suggest that slightly deeper lines of dipoles in this area might be advisable. The extrapolated field shows no unreasonable oscillation. Also shown in Figure 6 is the first vertical derivative analytically computed every 5.35 km from the final lines-of-dipoles distribution. As expected, relatively local anomalies are sharpened; minor oscillations (e.g., between 190 km and 230 km) in the first vertical derivative reflect minor instabilities in the calculated dipole moments per unit length (not shown). Slightly shallower lines of dipoles in these areas would subdue these unwanted oscillations.

Results of upward-continuation of the observed field to 5 km and its reduction to the pole are shown in Figure 7; both fields are calculated every

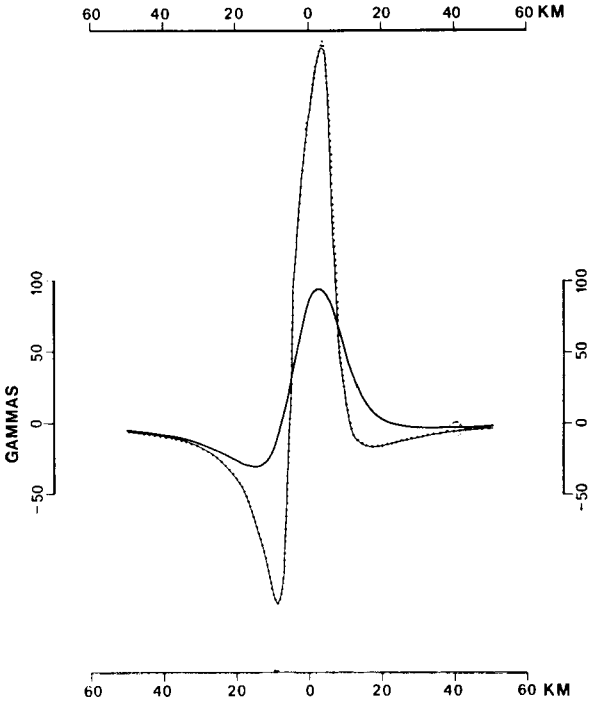

FIG. 3. Thick solid line (lower amplitude profile) is upward-continued (5 km) field due to both the theoretical prism and the final lines-of-dipoles distribution. Thin solid line and dotted line present comparison between downward-continued (1 km) fields due to both the prism and the final lines-of-dipoles distribution.

5.35 km. The original field is only slightly altered by reduction to the pole because of the relatively large inclination (68°N) involved.

The central trough present in the field profile (Figure 6) and the upward-continued profile (Figure 7) indicates a large amount of low-frequency content. This is more explicitly shown in the amplitude spectrum as analytically calculated from the final lines-of-dipoles distribution. Figure 8 shows this spectrum compared to that obtained by a standard fast Fourier transform technique. The difference in frequency content of the lines-of-dipoles amplitude spectrum reflects the lack of rigorous control at the interpolation and extrapolation points; that is, the lines-of-dipoles spectrum represents the frequency content of that analytic field over all space. It is apparent from Figure 8 that high-passing the field between limits of 0.006 and ∞ cycles/km will eliminate significant low-frequency content. The result of applying such a high-pass filter to the observed profile is shown in Figure 9 along with the difference between it and the original profile.

DISCUSSION

The above presentation is designed to show that the equivalent-source technique is a valid method for processing two-dimensional magnetic fields. However, as with all such methods, it has limitations. For example, abrupt changes in the character of a profile or presence of somewhat equal high- and low-frequency components will prohibit location of all sources at the same depth, because poor interpolation and/or unstable source amplitudes will result. Such profiles can be handled theoretically by varying both magnitude and location parameters for a large number of lines of dipoles (Zidarov, 1965). In practice, such a nonlinear problem greatly increases computation time and is more susceptible to computation instabilities. Another possible approach is to fix each equivalent source at a certain depth, judiciously chosen on the basis of the general character of the field above that source, and then solve the linear inverse problem. Such an approach would be feasible for relatively simple profiles (e.g., the field example above), but choice of individual

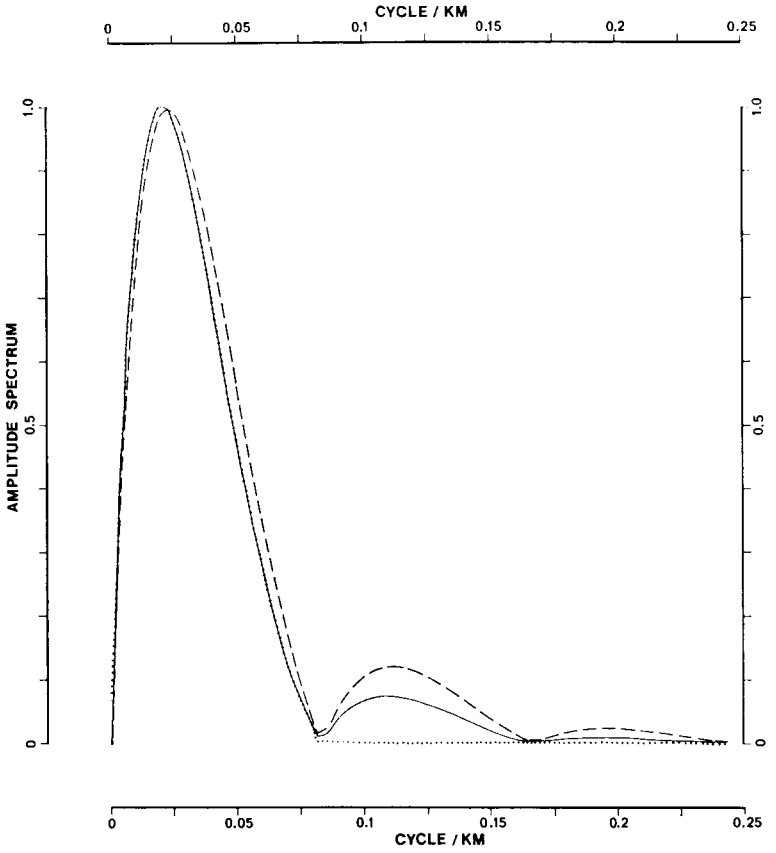

FIG. 4. Solid line is amplitude spectrum of prism field before band-passing, obtained by both a standard fast Fourier transform technique and from the final lines-of-dipoles distribution. Although a single solid line is used to represent both spectra, they do differ slightly; that is, the former as a value of 0.065 units for zero frequency while the latter has no zero frequency content. Dashed line is amplitude spectrum of original prism field (downward-continued 1 km) obtained from the final lines-of-dipoles distribution. Dotted line is amplitude spectrum of prism field after band-passing, obtained by a standard fast Fourier transform technique.

depths when processing more complex profiles would be rather ambiguous. Needham (1970) extensively discussed the problem of locating individual equivalent sources (point masses).

On the positive side, when applicable, the technique allows certain processing to be done on the basis of a single operation; i.e., solution of the inverse problem to obtain the equivalent-source distribution. If the processing were done using separate techniques available in the literature, the individual limitations and idiosyncrasies of each technique would have to be considered separately.

The equivalent-source technique for reduction to the pole is easily extended to handle cases where remanent magnetization is present and its directional properties are known. That is, the equivalent sources used, whether they are lines of dipoles, lines of poles, two-dimensional rectangular prisms, etc., are assumed to possess the same remanence properties as the true geological sources. The method also allows reduction to the pole of fields observed at any magnetic latitude.

The amplitude spectrum and band-passed field, when analytically calculated as above, must be viewed with caution. The formulas for these quantities represent the theoretical field of the equivalent sources over all space, and not just at the locations of the observed field values on the basis of which those sources were determined. It is therefore advisable to calculate the final equivalent source field at both interpolation and extrapolation points to be sure that no unrealistic behavior of the theoretical field at these points will

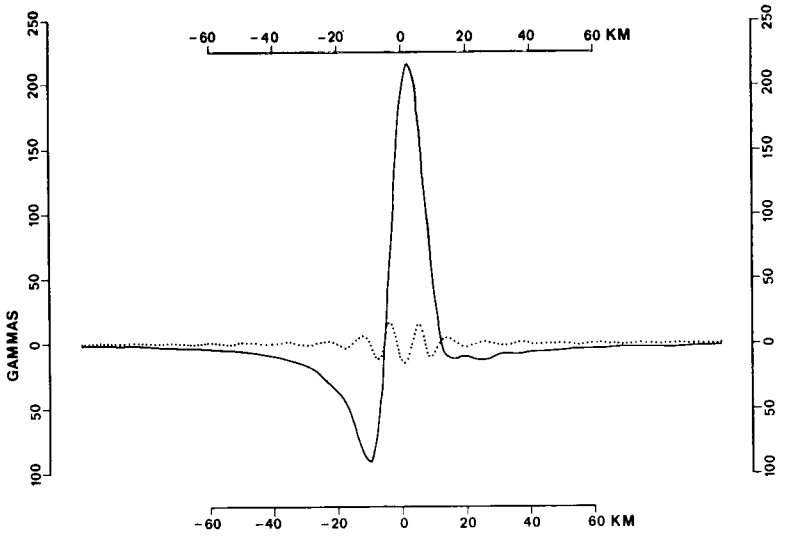

FIG. 5. Solid line is low-pass field obtained from the prism field using the final lines-of-dipoles distribution. Dotted line is the difference between the low-pass field and the original field.

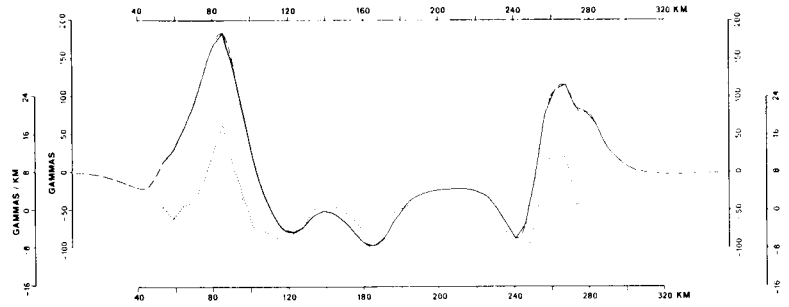

FIG. 6. Solid line is observed total magnetic field profile; dashed line is field due to final lines-of-dipoles distribution obtained by solution of the inverse magnetic problem. Dotted line is first vertical derivative field calculated from final lines-of-dipoles distribution.

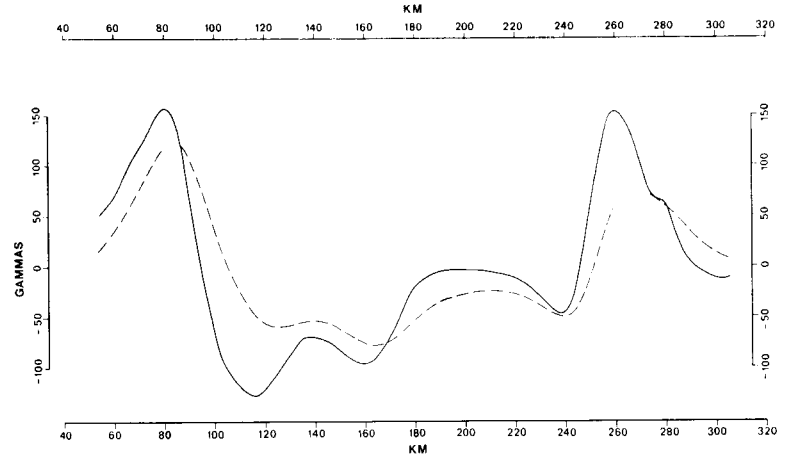

FIG. 7. Solid and dashed lines are, respectively, the observed field reduced to the pole and upward-continued to 5 km using the final lines-of-dipoles distribution.

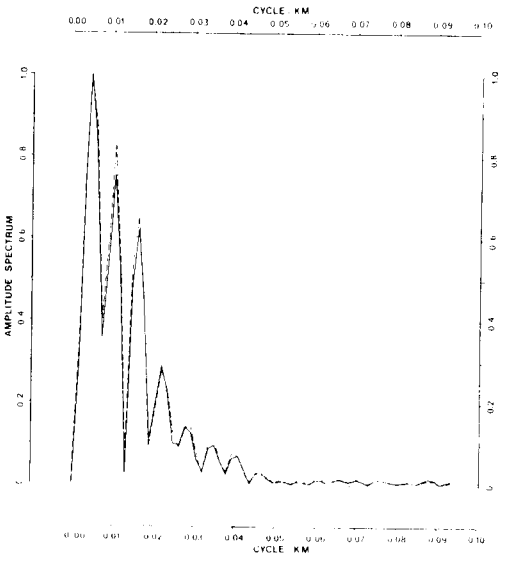

FIG. 8. Solid and dashed lines are, respectively, the amplitude spectrum of the observed field obtained by standard fast Fourier transform technique and the amplitude spectrum of the observed field obtained from the final lines-of-dipoles distribution.

adversely affect the amplitude spectrum or band-passed field.

CONCLUSION

The equivalent-source technique has been shown to be quite useful in processing total magnetic field profiles; extension to the field measured on a surface is straightforward. It is a unified and concise method with a sound analytic base that is quite easy to use in many cases. The increasingly large number of institutions possessing inverse modeling capability, therefore, have the inherent capability of further processing the observed fields without having to set up unrelated routines and procedures for each process.

ACKNOWLEDGMENTS

The author is indebted to Robert L. Massey of Marathon Oil Company, Denver Research Center, Littleton, Colorado, who did the programming and made many valuable suggestions during the course of this work. Sincere thanks are extended to Professor Gunnar Bodvarsson, Departments of Mathematics and Oceanography, Oregon State University, for reviewing this paper.

Permission from Marathon Oil Company management to publish this work is appreciated.

REFERENCES

Anonymous, 1968, Metrication in scientific journals: Am. Sci., v. 56, p. 159–164.

Baranov, V., 1957, A new method for interpretation of aeromagnetic maps: Pseudo-gravimetric anomalies: Geophysics, v. 22, p. 359–383.

Bhattacharyya, B. K., 1965, Two-dimensional harmonic analysis as a tool for magnetic interpretation: Geophysics, v. 30, p. 829–857.

Bodvarsson, G., 1971, Approximation methods for equivalent strata: J. Geophys. Res., v. 76, p. 3932–3939.

Bott, M. H. P., 1967, Solution of the linear inverse problem in magnetic interpretation with application to oceanic magnetic anomalies: Geophys. J. R. Astr. Soc., v. 13, p. 313–323.

Bott, M. H. P., and Hutton, M. A., 1970 a, A matrix method for interpreting oceanic magnetic anomalies: Geophys. J. R. Astr. Soc., v. 20, p. 149–157.

——— 1970 b, Limitations on the resolution possible in the direct interpretation of marine magnetic anomalies: Earth and Planetary Sci. Ltrs., v. 8, p. 317–319.

Brakl, J., Clay, C. S., and Rona, P. A., 1968, Interpretation of a magnetic anomaly on the continental rise off Cape Hatteras: J. Geophys. Res., v. 73, p. 5313–5315.

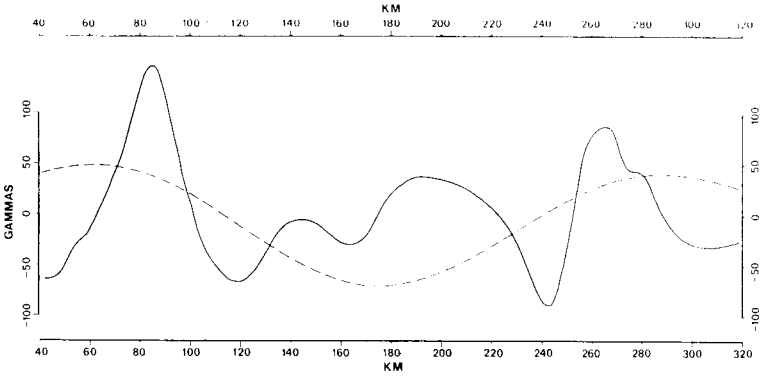

FIG. 9. Solid line is the high-pass field obtained from the final lines-of-dipoles distribution; dashed line is the difference between the high-pass field and the observed field.

Bullard, E. C. and Cooper, R. I. B., 1948, The determination of masses necessary to produce a given gravitational field: Proc. Roy. Soc. Lon. A, v. 194, p. 332–347.
Corbato, C. E., 1965, A least-squares procedure for gravity interpretation: Geophysics, v. 30, p. 228–233.
Dampney, C. N. G., 1969, The equivalent source technique: Geophysics, v. 34, p. 39–53.
Emilia, D. A. and Bodvarsson, G., 1969, Numerical methods in the direct interpretation of marine magnetic anomalies: Earth and Planetary Sci. Ltrs., v. 7, p. 194–200.
———— 1970, More on the direct interpretation of magnetic anomalies: Earth and Planetary Sci. Ltrs., v. 8, p. 320–321.
Emilia, D. A., Heinrichs, D. F., Brakl, J., Clay, C. S., and Rona, P. A., 1972, Re-interpretation of a magnetic anomaly on the continental rise off Cape Hatteras: J. Geophys. Res., v. 77, p. 377–379.
Hahn, A., 1965, Two applications of Fourier's analysis for the interpretation of geomagnetic anomalies: J. Geomag. Geoelec., v. 17, p. 195–225.
Hall, D. H., 1958, Least squares in magnetic and gravity interpretation: Trans. Am. Geophys. Union, v. 39, p. 35–39.
Henderson, R. G., 1970, On the validity of the use of the upward-continuation integral for total magnetic intensity data: Geophysics, v. 35, p. 916–919.
Johnson, W. W., 1969, A least-squares method of interpreting magnetic anomalies caused by two-dimensional structures: Geophysics, v. 34, p. 65–74.
Needham, P. E., 1970, The formation and evaluation of detailed geopotential models based on point masses: Ohio State Univ. Dept. of Geod. Sci. Rep. No. 149, 253 p.
Strakhov, V. N., 1969, Approximate solution of incorrectly posed linear problems in Hilbert space with applications to exploration geophysics: Acad. of Sci., USSR, Phys. of the Solid Earth (Eng. ed.), no. 8, p. 495–506.
Zidarov, D., 1965, Solution of some inverse problems of applied geophysics: Geophys. Prosp., v. 13, p. 240–246.

APPENDIX

The equivalent-source (lines-of-dipoles) configuration used in this paper is shown in Figure A1. The infinite lines of dipoles, obtained by solution of the linear inverse problem, are perpendicular to the observed field profile and lie on a plane h km below the plane ($z=0$) of observation. Induced magnetic properties are assumed and pertinent angles are shown in Figure A2. We use SI or MKSA units (Anonymous, 1968).

The total magnetic field at the jth point of calculation due to n lines of dipoles is

$$F_j \text{ (gammas)} = \sum_{k=1}^{n} M_k G_{jk} \qquad \text{(A1)}$$

(1 gamma $= 10^{-9}$ Weber/m$^2 = 10^{-9}$ tesla),

where M_k = dipole moment unit length (ampmeter) of the kth line of dipoles;

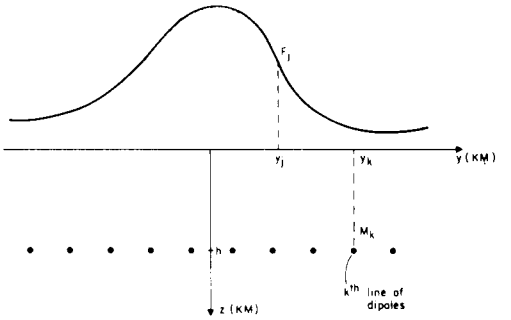

FIG. A1. Lines-of-dipoles configuration used in this paper. The profile actually represents any of the quantities calculated from the final lines-of-dipoles distribution.

$$G_{jk} = \frac{2 \times 10^{-7} A_2^2}{L_{jk}^4} \{2(A_1^2 y_{jk}^2 - 2A_1 y_{jk} h + h^2) - (A_1^2 + 1) L_{jk}^2\};$$

$A_1 = \cot I \sin \beta$;

$A_2 = \sin I$;

$y_{jk} = y_j - y_k$;

y_j = lateral position in kilometers of the jth magnetic field value (F_j);

y_k = lateral position in kilometers of the kth line of dipoles; and

$L_{jk}^2 = y_{jk}^2 + h^2$.

This equation is used to calculate the upward- and downward-continued field by merely changing the value of h.

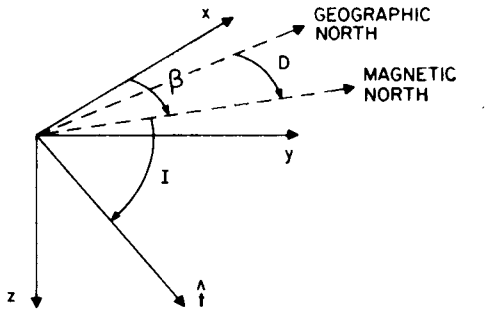

FIG. A2. Coordinate system and angles used in lines-of-dipole calculations. I and D are the inclination and declination of the regional geomagnetic field and $\mathbf{t}$ is the unit vector in the direction of that field. The total magnetic field profile is along the y-axis.

The first vertical derivative is

$$PF_j \text{ (gammas/km)} = \sum_{k=1}^{n} M_k(PG)_{jk}, \quad \text{(A2)}$$

where

$$(PG)_{jk} = \frac{4 \times 10^{-4} A_2^2}{L_{jk}^6} \{[2A_1 y_{jk} - (A_1^2 + 3)h]L_{jk}^2 + 4h[A_1^2 y_{jk}^2 - 2A_1 y_{jk} h + h^2]\}.$$

The second vertical derivative field is

$$PPF_j \text{ (gammas/km}^2) = \sum_{k=1}^{n} M_k(PPG)_{jk}, \quad \text{(A3)}$$

where

$$(PPG)_{jk} = \frac{4 \times 10^{-4} A_2^2}{L_{jk}^8} \{[A_1^2 + 3]L_{jk}^4 - 4[A_1^2 L_{jk}^2 - 6h(A_1 y_{jk} - h)]L_{jk}^2 + 24h^2[A_1^2 y_{jk}^2 - 2A_1 y_{jk} h + h^2]\}.$$

The Fourier transform pair of the lines-of-dipoles field calculated along the y-axis is defined as

$$f(\omega) = \int_{-\infty}^{\infty} F_j(y) e^{-i\omega y} dy = R(\omega) + iI(\omega),$$

and

$$F_j(y) = \frac{1}{2\pi} \int_{-\infty}^{\infty} f(\omega) e^{i\omega y} d\omega,$$

where

ω = angular frequency;

$R(\omega)$ = real part of $f(\omega)$;

and

$I(\omega)$ = imaginary part of $f(\omega)$.

The amplitude spectrum of F_j for $\omega \geq 0$ is, therefore,

$$A(\omega) = [R^2(\omega) + I^2(\omega)]^{1/2} = 4\pi \times 10^{-4} A_2^2 e^{-\omega h} \cdot \left\{ \left[\sum_{k=1}^{n} M_k(2A_1 \omega \sin \omega y_k - A_1^2 \omega \cos \omega y_k + \omega \cos \omega y_k) \right]^2 + \left[\sum_{k=1}^{n} M_k(2A_1 \omega \cos \omega y_k + A_1^2 \omega \sin \omega y_k - \omega \sin \omega y_k) \right]^2 \right\}^{1/2}. \quad \text{(A4)}$$

The equation for F_j band-passed between angular frequency limits ω_1 and $\omega_2 (\omega_2 > \omega_1)$ is

$$BPF_j = \frac{1}{2\pi} \left[\int_{-\omega_2}^{-\omega_1} f(\omega) e^{i\omega y} d\omega + \int_{\omega_1}^{\omega_2} f(\omega) e^{i\omega y} d\omega \right] = \sum_{k=1}^{n} M_k(BPG)_{jk}, \quad \text{(A5)}$$

where

$$(BPG)_{jk} = 2 \times 10^{-4} A_2^2 \frac{e^{-\omega h}}{L_{jk}^2} \left\{ (1 - A_1^2) \cdot \left[\omega(y_{jk} \sin \omega y_{jk} - h \cos \omega y_{jk}) - \frac{1}{L_{jk}^2} (S_{jk} \cos \omega y_{jk} - 2y_{jk} h \sin \omega y_{jk}) \right] + 2A_1 \left[\omega(h \sin \omega y_{jk} + y_{jk} \cos \omega y_{jk}) + \frac{1}{L_{jk}^2} (S_{jk} \sin \omega y_{jk} + 2y_{jk} h \cos \omega y_{jk}) \right] \right\} \Bigg|_{\omega_1}^{\omega_2},$$

where

$$S_{jk} = h^2 - y_{jk}^2;$$

and

$$f(\omega) \Big|_{\omega_1}^{\omega_2} = f(\omega_2) - f(\omega_1).$$